LITHOLOGICAL MAPPING OF OPHIOLITE COMPLEX WITH EMPHASIS ON CHROMITE AND MAGNESITE EXPLORATION USING REMOTE SENSING TECHNIQUES

MOHSEN POURNAMDARI

A thesis submitted in fulfilment of the
requirements for the award of the degree of
Doctor of Philosophy (Remote Sensing)

Faculty of Geoinformation and Real Estate
Universiti Teknologi Malaysia

JANUARY 2014

"To my beloved wife and son"

ACKNOWLEDGEMENT

I would like to express my special appreciation and thanks to my supervisor Prof. Dr. Mazlan Bin Hashim, you have been a tremendous mentor for me. I would like to thank you for encouraging my research and for allowing me to grow as a research scientist. Your advice on both research as well as on my career have been invaluable. At the same time, I would like to extend my appreciation to Universiti Teknologi Malaysia for International Doctorate Fellowship (IDF) award.

A special thanks to my family. Words cannot express how grateful I am to my family. Your prayer for me was what sustained me thus far.

I would also like to thank my beloved wife, Zahra. Thank you for supporting me, and especially I cannot thank you enough for encouraging me throughout this experience. To my beloved son, Parham, I would like to express my thanks for being such a good boy always cheering me up. I will keep on trusting you for my future.

ABSTRACT

This research employed the Advanced Spaceborne Thermal Emission and Reflection Radiometer (ASTER) and Landsat Thematic Mapper (TM) data for lithological mapping and delineating of high potential chromite zone mineralization in ophiolite complexes. Abdasht, Soghan and Sikhoran chromite mining areas located in Sanandaj-Sirjan technically a part of the Esphandagheh ophiolite complex zone in Kerman province, southeastern of Iran have been selected for this research. In order to discriminate and to demarcate of the high potential chromite and magnesite rock zone, ASTER and Landsat TM bands properties have been utilized for running principal components analysis (PCA), band ratio (BR), minimum noise fraction (MNF), de-correlation stretch, log residual, spectral mapping methods and feature level fusion. A comparison between the image processing results with field investigation and primary geological map confirmed the concentration of chromite and magnesite mineralized zone associated with serpentinized dunite and hurzburgite. A new geological map showing high potential chromite zones and the boundary of lithological units was produced based on the interpretation of remote sensing data. The map can be used for geological exploration and mine engineering purposes. The data and methods used have emphasized high ability of the ASTER data to provide geological information for detecting chromite host rock such as serpentinized dunites and hurzburgite as well as lithological mapping at both district and regional scales. Additionally, Landsat TM data have also produced suitable results for lithological purposes on a regional scale. The approach used in this study is broadly applicable for exploring new chromite prospects and lithological mapping of the ophiolitic complexes especially in the arid and semi-arid regions of the earth.

ABSTRAK

Penyelidikan ini membincangkan data Advanced Spaceborne Thermal Emission and Reflection Radiometer (ASTER) dan Landsat Thematic Mapper(TM) untuk pemetaan litologi dan menggambarkan zon mineral kromit berpotensi tinggi ofiolit kompleks. Abdasht, Soghan dan Sikhoran ialah kawasan perlombongan kromit terletak di Sanandaj-Sirjan yang secara teknikalnya merupakan sebahagian daripada zon Esphandagheh ofiolit kompleks di daerah Kerman, tenggara Iran telah dipilih untuk kajian ini. Untuk membezakan batu dan menentukan sempadan kromit berpotensi tinggi dan zon batu magnesit, ciri-ciri band ASTER dan Landsat TM telah digunakan untuk mengendalikan analisis komponen utama (PCA), nisbah band (BR), pecahan bunyi minimum (MNF), rentang dikorelasi, log sisa, kaedah pemetaan spektral dan lakuran paras ciri. Perbandingan antara keputusan pemprosesan imej dengan kerja lapangan dan peta geologi mengesahkan bahawa tumpuan kromit dan zon mineral magnesit berkaitan dengan serpentinized dunite dan hurzburgite. Peta geologi yang baharu telah menunjukkan zon kromit berpotensi tinggi dan sempadan unit-unit litologi telah dihasilkan berdasarkan tafsiran data penderiaan jarak jauh. Peta ini boleh digunakan untuk penerokaan geologi dan tujuan kejuruteraan perlombongan. Data dan metodologi yang digunakan telah menekankan tentang kemahiran tinggi data ASTER dalam menyediakan maklumat geologi untuk mengesan batuan kromit seperti serpentinized dunite dan hurzburgite serta peta litologi di kedua-dua daerah dan skala kawasan. Selain itu, data Landsat TM telah menghasilkan keputusan yang sesuai untuk tujuan litologikal di skala kawasan. Pendekatan dalam kajian ini secara umumnya dapat digunakan untuk meneroka prospek kromit baharu dan pemetaan litologi ofiolit kompleks terutamanya di kawasan gersang dan separa gersang bumi.

TABLE OF CONTENTS

LIST OF TABLES

LIST OF FIGURES

LIST OF ABBREVIATIONS

MSS	-	Landsat Multi Spectral Scanner
ETM	-	Landsat Enhanced Thematic Mapper
TM	-	Landsat Thematic Mapper
NASA	-	National Aeronautics and Space Administration
METI	-	Ministry of Economy, Trade and Industry
VNIR	-	Visible Infrared
SWIR	-	Short-Wave Infrared
TIR	-	Thermal Infrared
EOSDIS	-	Science Component and Data Information System
ASTER	-	Advanced Spaceborne Thermal Emission and Reflection Radiometer
PCA	-	Principal Component Analysis
MNF	-	Minimum Noise Fraction
BR	-	Band Ratio
SAM	-	Spectral Angle Mapper
MTMF	-	Mixture Tuned Matched Filtering
OIF	-	Optimum Index Factor
XRD	-	X-Ray Diffraction
ASD	-	Analytical Spectral Devices
MF	-	Match Filtering
SFF	-	Spectral Features Fitting
LSU	-	Linear Spectral Unmixing
RGB	-	Red - Green - Blue
FFT	-	Fact Fourier Transform
FCC	-	Fast Color Composite
MLL	-	Maximum Likelihood
SID	-	Spectral Information Divergence

QI	-	Quarts Index
CI	-	Carbonate Index
MI	-	Mafic Index
MOR	-	Middle Ocean Rift
EOS	-	Earth Observing System
SID	-	Spectral Information Divergence
ERSDA	-	Earth and Remote Sensing Data Analysis Center
JHU	-	Johns Hopkins University
JPL	-	Jet Propulsion Laboratory
USGS	-	United States Geological Survey
AIG	-	Analytical Imaging and Geophysics

LIST OF APPENDICES

CHAPTER 1

INTRODUCTION

1.1 Research Background

Remote Sensing technology applications have been widely used in various aspects of science such as geology, geography, archaeology and environmental studies. In recent years, geologists and mining engineers have used remote sensing technology in the exploration of minerals, new ore deposits, oil-exploration, lithological mapping and environmental geology. Mineral resources play a vital role in the economic development of countries. Due to extraordinary growing of demands for mineral, the depleted resources must be replaced with new resources.

Therefore, the remote sensing technology can increase the exploration of minerals and new ore deposits. It is suitable for collecting the data from large areas using advanced sensors, mounted on a satellite or aircraft systems. Remote sensing technologies play an important role in the early stages of ore exploration especially in arid and semi-arid areas, where the surface of the terrain is mostly bare or covered with little vegetation. Geological maps with their subsequent derivative are considered to be the most reliable geosciences information having immense economic and societal value.

In addition, a geological map is able to supply information about not only the dispensation and thickness of exclusive rock units but also shows relationship and structures, which provide insight to characteristic of mineral potential zones. In today's world, getting geological information are greatly supported by remote sensing data and methods that, have been done already. In addition, the traditional techniques for geological mapping have problems such as limited exposed outcrop, time and cost consuming. Ophiolite complexes belts located in continental crust are usually assumed markers of suture zones. The ophiolites are simply a part of the oceanic crust and the underlying mantle, which have been raised higher and set up an exhibition into the continental crust rocks.

Initially, the ophiolite complex was determined as a gathering of mafic and ultra-mafic rock units (Anonymous, 1972). Ophio is the Greek word for “snake” lite means “stone’’from the Greek lithos. From the lowest layers to the higher layers, the different sequence of ophiolie complex involved ultra-mafic rock units (lherzolite, harzburgite, dunite and gabbro), mafic rocks (sheeted dicks and pillow lavas) and associated rock units such as sedimentary and carbonate rocks.

In addition, the study of ophiolite complex is a great opportunity for understanding the amalgamation of early oceanic crust and continental crust processes (Shervais, 1993; Moore *et al*., 2008). The metamorphic rocks, which occurred in a particular place specifically under the harzburgite layers, have a thickness around 500 m and show a reversed metamorphism (Williams and Smyth, 1973). It is proved that, this metamorphism happened during the uplifting and replacement of hot oceanic crust to continental crust or during the abduction process (Williams and Smyth, 1973; Casey and Dewey, 1984; Shervais, 1993).

Over the past years, the satellite data widely have been employed in mineral exploration and geology studies (Bishop *et al*., 2011; Carranza and Hall, 2002; Crowley *et al*., 1989; Kruse *et al*., 1999; Sultan *et al*., 1986). The Landsat thematic mapper (TM) and an enhanced thematic mapper (ETM^+) including six spectral bands between the visible (VNIR), shortwave (SWIR) and involve one thermal infrared (TIR) portion of the electromagnetic spectrum are suitable for geology studies and exploration of new source of ore deposits. Using of Landsat satellite data began on Landsat 4 and then provides several developments over the MSS sensor such as increasing the radiometric, spatial and spectral resolution. And also the number of directors in each band increased.

The spatial resolution of VNIR, SWIR and TIR bands of Landsat TM are 30 m and 120 m respectively. The last Landsat satellites launched at around 700 km in 16 days revisit periods. The Landsat multi spectral scanner (MSS) and Landsat thematic mapper (TM) with seven spectral bands, have been employed for lithological mapping and geological studies in regional scale (Goetz and Rowan, 1983; Goetz, 2009; Sultan *et al*., 1987; Tangestani and Moore, 2000; Kavak, 2005; Krohn *et al*., 1978; Raines, 1978; Kusky and Ramadan, 2002; Perry, 2004; Rajesh, 2008; Sabins, 1996; Sabins, 1997).

Unprecedented opportunity for exploration geologist in order to explore ophiolite complex related to chromite and magnesite ore deposits with remote sensing data has been created with the launch of the Landsat TM launched by NASA in 1972 and the Advanced Space borne thermal Emission and Reflection Radiometer (ASTER) on 18 December 1999. Table 1.1 shows the characteristics of Landsat TM and some valuable applications of each.

Table 1.1: Characteristic of Landsat TM satellite data

Landsat 4-5	Wavelength Range (µm)	Applications	Resolution (m)
Band 1	0.45-0.52 (blue)	Soil/ vegetation discrimination/bathymetry/coastal mapping-urban feature identification	30
Band 2	0.52-0.60 (green)	Green vegetation mapping/cultural/urban feature identification	30
Band 3	0.63-0.69 (red)	Vegetated vs. non vegetated and plant species discrimination (plant chlorophyll absorption) / cultural/urban feature identification	30
Band 4	0.76-0.90 (near IR)	Identification of plant/ vegetation type , health, and biomass content/water body delineation , soil moisture	30
Band 5	1.55-1.75 (Short Wave)	Sensitive to moisture in soil and vegetation/ discriminating snow and cloud covered area	30
Band 6	10.4-12.5 (Thermal IR)	Vegetation stress and soil moisture discrimination related to thermal radiation/thermal mapping (urban water)	(120)*30
Band 7	2.08-2.35 (Short Wave IR)	Discrimination of mineral and rock types/sensitive to moisture content	30

* TM Band 6 was acquired at 120-meter resolution, but products processed before February 25, 2010 are resample to 60-meter pixels. Products processed after February 25, 2010 are resample to 30-meter pixels (Abdeen *et al.*, 2001).

ASTER is a new sensor with improved abilities for geology studies and mineral exploration that was made by Japan's METI and inaugurate by NASA on EOS/Terra platform. ASTER with 14 bands as a multi-spectral sensor, which is able to identify the reflected and emitted radiation from earth and the atmosphere. In addition, the ASTER has three kinds of bands including three visible (VNIR), six shortwave (SWIR) and five thermal (TIR) bands with 0.52 and 0.86 μm and 15m spatial resolution, 1.6 to 2.43 μm and 30m spatial resolution and 8.125-11.65 μm wavelength and 90m resolution respectively (Yamaguchi *et al.*, 1999; Abrams, 2000).

The swath width of ASTER in every single scene (60×60 km) is 60 km that makes it suitable for lithological mapping in regional scale (Table1.2). One of the series of multi device typing NASA earth-observing system is Terra which, including science component and a data information system (EOSDIS). The type of Terra is polar orbiting and low tendency for long time observation land surface for study atmosphere, biosphere and oceans. The crosstalk correction algorithm and atmospheric correction have been pre-applied to the ASTER level 1B data (Iwasaki and Tonooka, 2005; Biggar *et al.*, 2005; Mars and Rowan, 2010).

The six spectral bands of the ASTER shortwave infrared radiation subsystem were designed to measure reflected solar radiation in order to distinguish Al-OH, Fe, Mg-OH, Si-O-H, and CO_3 absorption features (Abrams and Hook, 1995; Fujisada, 1995). The use of ASTER multispectral data has increased in exploration and lithological mapping in recent years. Due to the spectral characteristics of the ASTER bands unique integral is very sensitive to mineralogy, particularly in the visible and the shortwave infrared region, the applicability of the diversity of image processing, "on demand " availability of data at low cost and broad coverage for mapping at the regional level.

The capabilities of ASTER satellite data are like other high spatial resolution satellite, these include: (a) climatology; (b) study of vegetation's; (c) volcanic activities monitoring; (d) hazards monitoring; (e) hydrology; (f) geology and soils as well as (g) land cover change. This application is primarily due to the ability of the sensor, and based on the characteristics of the spectral signatures and other geological features related to the mineral ore deposits record (Ducart *et al.*, 2006). Figure 1.1 shows similarities and differences between the spectral bands of ASTER and Landsat ETM^{+}.

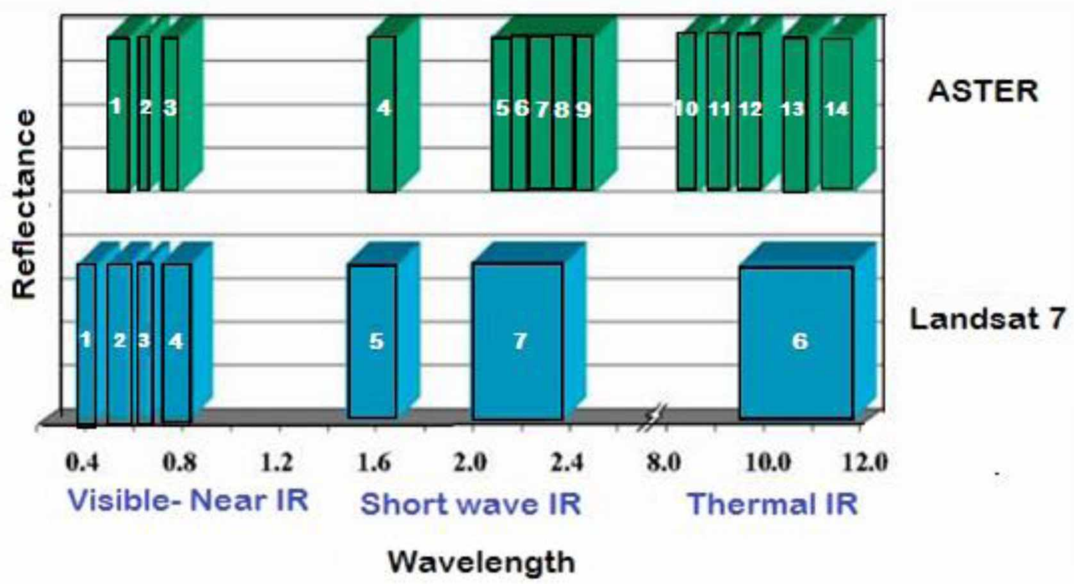

Figure 1.1 Comparison of spectral bands between ASTER and Landsat 7 (Abrams *et al.*, 2004)

Table 1.2: The technical characteristics of ASTER data (Fujisada, 1995; Yamaguchi *et al.*, 1999)

Subsystem	**Band number**	**Spectral range (µm)**	**Radiometric resolution**	**Absolute accuracy(σ)**	**Spatial resolution**	**Signal quantization levels**
VNIR	1	0.52-0.60	NE Δρ ≤ 0.5%	≤ 4%	15 m	8 bits
	2	0.63-0.69				
	3N	0.78-0.86				
	3B	0.78-0.86				
SWIR	4	1.600-1.700	NE Δρ ≤ 0.5%			
	5	2.145-2.185	NE Δρ ≤ 1.3%			
	6	2.185-2.225	NE Δρ ≤ 1.3%	≤ 4%	30 m	8 bits
	7	2.235-2.285	NE Δρ ≤ 1.3%			
	8	2.295-2.365	NE Δρ ≤ 1.0%			
	9	2.360-2.430	NE Δρ ≤ 1.3%			
TIR	10	8.125-8.475		≤ 3K (200-240K)		
	11	8.475-8.825		≤ 2K (240-270K)	90 m	12 bits
	12	8.925-9.275	NE ΔT ≤ 0.3%	≤ 1K (270-340K)		
	13	10.25-10.95		≤ 2K (340-370K)		
	14	10.95-11.65				

Stereo base-to-height ratio 0.6 (along-track)
Swath width 60 km
Total coverage in cross-track direction by pointing 232 km
Coverage interval 16 days
Altitude 705 km
MTF at Nyquist frequency 0.25 (cross-track) 0.20 (along-track)
Band to band registration Intra-telescope: 0.2 pixels Intra-telescope: 0.3 pixels
Peak power 726 w
Mass 406 kg
Peak data rate 89.2 Mbps
Band number 3N refers to the nadir pointing view, whereas 3B designates the backward pointing view.

Research on ophiolite complexes have been done with traditional techniques in Iran. Lithological mapping of ophiolite complex in the normal range for a long time can be made difficult and expensive when looking at large areas where the field is also troublesome to access necessary. As a result, the rock units in ophiolite complex are often assigned to regional scales, resulting in maps; the lithological connections are widespread in many cases vague. The chromite ore deposit is one of the most significant minerals, which have been developed using satellite imagery in the last 15 years. Since ophiolites are an important part of the oceanic earth crust having many chromite deposits, they are suitable case studies to be considered in the area of remote sensing research.

The main goal of this research is to investigate about the relationship between lithology and structure of the rock units in the study area with emphasize on exploration of chromite and magnesite bearing mineralized zones and interpreting the information contained in various data sets can result in producing necessary information related to lithological map using remote sensing data. In this study, ophiolite complexes located in south of Iran were selected as a case study area. This area has not been studied using remote sensing techniques.

Satellite remote sensing methods are a tool for detailed geological analysis, especially in less accessible areas of the earth. Using remote sensing satellite data, for instance aerial photographs and satellite imagery are normally included in lithological mapping programs to get geological information, which is the best displayed by overhead perspectives. A number of researches have shown that, the remote sensing hyperspectral satellites data are able to map and explore the spectrally distinct mafic and ultra-mafic minerals, which are significant in different industries (Crowley *et al.*, 1989; Crowley and Clark, 1992; Kruse *et al.*, 1993; Boardman *et al.*, 1995; Crosta *et al.*, 2003; Cock *et al.*, 1998; Kruse *et al.*, 1999; Kruse *et al.*, 2003; Kruse *et al.*, 2003; Perry, 2007; Gersman *et al.*, 2008; Bedini *et al.*, 2009).

1.2 Statements of Problem

Ophiolites complex present an excellent opportunity for studying oceanic crust and can be the best candidate for mapping complex lithology using remote sensing satellite data. In addition, these rock formations are significant for exploration mineral resources, mainly for chromite and magnasite ore deposits. The current improvement of multi-spectral remote sensing devices, like ASTER and Landsat TM sensor, potentially suggest to geologists and mining engineers to employ remote sensing methods to reduce the cost and time-consuming for regional geological mapping and new source mineral exploration. Prior studies, which used traditional methods, are confronted with the follow problems in the study area:

- High diversity of mineral and rocks are observed in ophiolite complexes.
- Extensive and scattering scope of ophiolites complexes makes the process of study to be complicated.
- Ophiolitic regions are not easy to access because of geographical and geological positions.

These mentioned problems and characteristics of ophiolite complexes as an interesting part of the oceanic crust and use of traditional techniques for the study and exploration of chromite and magnesite shows that, the traditional methods are time and cost consuming. Current studies have focused on remote sensing techniques because of:

A) Accurate detection; B) Low cost and fast; C) Flexible and adaptable

Furthermore, existing methods are not able to show ophiolite complexes clearly and the fusion technique has not been used in prior studies. In addition, current methods cannot produce geological maps efficiently and in spite of having high potential magnesite and chromite areas. The Abdasht, Soghan and Sikhoran ophiolite complexes are selected as a case study in this investigation. At present, there is a outdated map and there is no detailed geological map for this area and there is no prior remote sensing studies regarding lithological mapping and the discrimination of high economic potential chromite bearing mineralized zones (Aboelkhair *et al*., 2010; Khan *et al*., 2007; Gad and Kuski, 2007; Amer *et al*., 2010; Rejendran *et al*., 2011; Pournamdari and Hashim, 2013).

1.3 Objective of the Study

The objectives of this research are:

a) To delineate the area of chromite and magnesite potential mineralized zone and host rock lithology using visible, short wave and thermal infrared bands of ASTER and Landsat TM;

b) To determine the most suitable image processing methods for lithological mapping and discriminating chromite and magnesite in high potential area;

c) To perform a comparative analysis on image processing methods using ASTER and Landsat TM for mapping ophiolite at regional and district scales;

d) To investigate the synergism of fused ASTER and Landsat TM for mapping ophiolite complex; and

e) To produce a detailed geological map of the study area using fused ASTER and Landsat TM data.

1.4 Research Questions

a) Can chromite potential mineralized zone related to host rock lithology be delineated using visible, short wave, thermal infrared bands of ASTER, and visible and short wave infrared bands of Landsat TM?

b) Can optimal image processing methods be determined for lithological mapping, discriminating chromium and magnesium in a high potential area?

c) Is it possible to perform a comparative analysis of image processing methods between ASTER and Landsat TM for mapping affiliate at regional and district scales?

d) Is it suitable to investigate the synergism of fused ASTER and Landsat TM for the mapping ophiolite complex?

e) Which remote sensing techniques are the most appropriate to produce the detailed geological map of the study area based on ASTER and Landsat TM data?

1.5 Scope of the Study

This study focusses on digital image processing for lithological mapping of ophiolite complex and delineating of chromite and magnesite in a high potential mineral zone using ASTER and Landsat TM satellite data. In addition, the relationship of ophiolite complex zones and chromite ore deposit regions are identified in the all ASTER and Landsat TM regions of the electromagnetic spectrum (VNIR, SWIR and TIR). The principal components analysis (PCA), band ratioing (BR), minimum noise fraction (MNF), decorrelation stretch and log residual are used to study ophiolite complexes.

Furthermore, lithology and the characteristics of ophiolite complexes are determined using image processing methods like the spectral angle mapper (SAM), feature level fusion and mixture tuned matched filtering (MTMF) on the shortwave infrared radiation subsystem of ASTER and Landsat TM data. In addition, to determine of better color composite in the image the two different ways including: correlation coefficient and the optimum index factor (OIF) method have been examined. The ASTER and Landsat TM images of the study area are processed and analyzed using ENVI and ERDAS software.

Laboratory experiments including X-Ray diffraction (XRD) and analytical spectral devices (ASD) are applied to collect rock samples to analyze bulk mineralogy and reflectance spectral. In addition, spectral reflectance measurements carried out using an analytical spectral device (ASD), which records a reflectance spectrum across an overall spectral range of 325–2500 nm (nanometer) with a 10 nm individual bandwidth. The measurements carried out in the remote sensing laboratory of the faculty of geoinformation and real estate, *Universiti Teknologi Malaysia (UTM)* using a non-contact probe and a "built-in illumination" source.

In order to achieve all mentioned purposes, Abdasht, Soghan and Sikhoran ophiolite complex located in the southeastern of Iran in Kerman province have been selected. The study area has a semi-arid climate where most of the earth's surface is well-exposed due to very sparse or bare due absence vegetation cover. The Abdasht ophiolite complex (56°46′ 42″ E, 28° 21′ 05″ N), Soghan ophiolite complex (56° 50' 73" E 28° 21' 60"N) and Sikhoran ophiolite complex (56° 58' 55" E, 28° 26' 36" N) are 130 km, 160 km and 185 km, far from Baft city and located in the arid and semi-arid regions respectively (Geological Survey of Iran, 1973; Modarres and Silva, 2007; Raziei *et al.*, 2005). Figure 1.2 shows the locations of the study area.

These ophiolite complexes are a part of the Esfandagheh mafic and ultra-mafic complexes (Paleozoic), which have been located in Sanandaj-Sirjan tectonically zone. In order to study the ophiolite complex related to chromite and magnesite and to achieve the research objectives, the ASTER and Landsat TM image sets were selected that, cover all the three Abdasht, Soghan and Sikhoran ophiolite complexes.

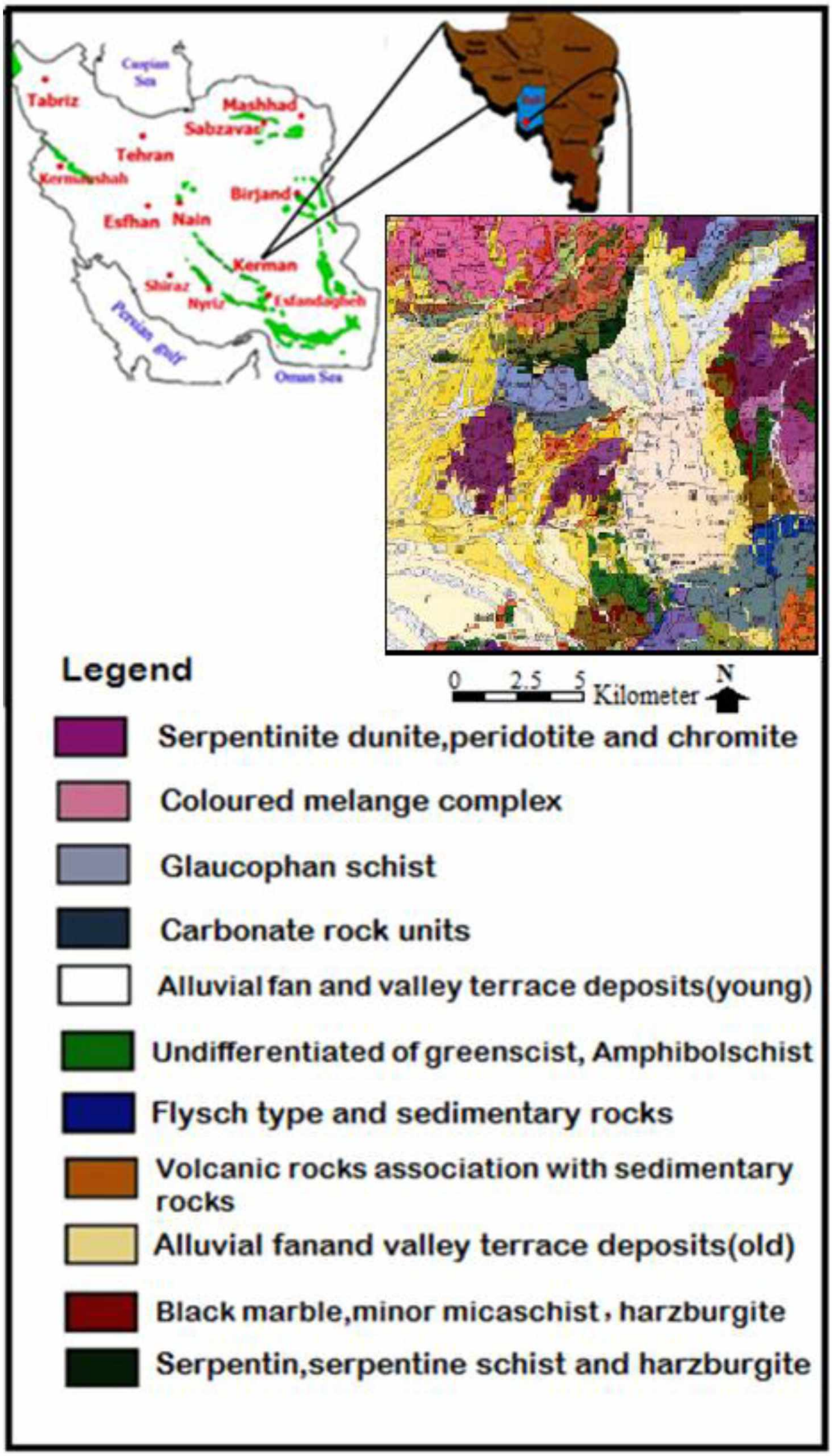

Figure 1.2 Location of study area

1.6 Novelty of the Study

In this section, the main differences between the current work and prior studies are elaborated. Based on the correlation coefficient results RGB images (7, 5, 1) and (5, 4, 1) of Landsat TM and (7, 4, 1), (7, 2, 1) and (1, 2, 3) of ASTER data give better color composite to visual of different lithology in the study area. The result of decorrelation stretch for bands 1, 2, 3 of the ASTER showed that, this technique is suitable for exploration of the chromite ore deposit. Using a log residual algorithm on VNIR+SWIR bands of ASTER data demonstrate ophiolite complexes at regional scale much better than SWIR bands of ASTER data. The result of the spectral angle mapper and MTMF method on ASTER and Landsat TM portrayed the location of serpentine dunite as the source of the chromite ore deposit and distribution of colored mélange complex in the study area.

In addition, the novel BR (4/1, 4/5, 4/7), the novel MNF (1, 2, 3) and the novel PCA (1, 2, 3) on ASTER data and the novel PCA (1, 3, 4), the novel MNF (1, 2, 3) on Landsat TM data are able to determining ophiolite complex rock units much better than previous reported methods in the study area. This research, based on the characteristic of multispectral sensors such as ASTER and Landsat TM satellite data showed that, the use of the feature level fusion technique prepared the good opportunity to study ophiolite complexes and lithological mapping.

1.7 Summary

This chapter summarized the basis and principles of research including an overview of the research topic, research background, problems to be solved through the current research, research questions and objectives, research domain as well as research justification. The above mentioned sections are considered as an introduction, which clarifies the different parts of the research. Indeed, the most important issues related to the current research were briefly explained to help readers obtain an overall understanding of the research components.

REFERENCES

Abdelsalam, M. and Stern, R. (2006). Mapping gossans in arid regions with Landsat TM and SIR-C images, the Beddaho Alteration Zone in northern Eritrea. *Journal of African Earth Sciences*, 30(4), 903-916.

Abdeen, M. M., Thurmond, A. K., Abdelsalam, M. G., Stern, R. J. (2001). Application of ASTER band-ratio images for geological mapping in arid regions; the Neoproterozoic Allaqi Suture, Egypt. *Geological Society of America*, 33, 1–289.

Aboelkhair, H., Yoshiki, N., Yasushi, W. and Isao S. (2010). Processing and interpretation of ASTER TIR data for mapping of rare-metal-enriched albite granitoids in the Central Eastern Desert of Egypt. *Journal of African Earth Sciences*, 58(1), 141-151.

Abrams, M.J., Brown, D., Lepley, L. and Sadowski, R. (1983). Remote sensing of porphyry copper deposits in Southern Arizona. *Economic Geology*, 78, 591-604.

Abrams, M.J. and Brown, D. (1984). Silver Bell, Arizona, porphyry copper test site report: Tulsa, Oklahoma, The American Association of Petroleum Geologists, The Joint NASA–Geosat Test Case Project, Final Report, chapter 4, p. 4-73.

Abrams, M. and Hook, S.J. (1995). Simulated ASTER data for geologic studies. *IEEE Transactions on Geoscience and Remote Sensing,* 33(3).

Abrams, M. (2000). The Advanced Spaceborne Thermal Emission and Reflection Radiometer (ASTER) data products for the high spatial resolution imager on NASA's Terra platform. *International Journal of Remote Sensing,* 21, 847-859.

Abrams, M., Hook, S. and Ramachandran, B. (2004). *ASTER User Handbook, Version 2.* Jet Propulsion Laboratory, California Institute of Technology. Online: http://asterweb.jpl.nasa.gov/content/03_data/04_Documents/aster_guide_v2.pdf.

Adams, M. J., Felic, A. L. (1967). spectrel reflectance 0.4-2.0 micron of silicate rock powder.*journal of geophysical research,* 72, 5705-5715.

Abdullah Mah (2002). Mapping surface cover types using Aster data.*GISdevelopment.net*

Ahmadipour, H. and Emami, M. (2003). "Soghan complex as an evidence for paleospreading center and mantle diapirism in Sanandaj-Sirjan zone (south-east Iran). *Journal of Sciences, Islamic Republic of Iran,* 14 (2).

Ackerman, R. (2009). A Bottom In Sight For chromite and magnesite Forbes. http://www.forbes.com/.

Adams, M. J., Felic, A. L. (1967). Spectrel reflectance 0.4-2.0 micron of silicate rock powder.*journal of geophysical research*, 72, 5705-5715.

Adams, J. B. (1974). Visible and near-infrared diffuse reflectance-spectra of pyroxenes as applied to remote sensing of soil objects in the solar system. *Journal of Geophysical Research*, 79 (1974), 4829–4836.

Adams, J.B., Smith, M.O. and Gillespie, A.R. (1983). Imaging spectroscopy Interpretation based on spectral mixture analysis. In: Pieters, C.M., Englert, P.A.J. (Eds.), *Remote geochemical analysis: Elemental and mineralogical composition*. Cambridge University Press, New York, 145-166.

Adams, J.B., Sabot, D.E., Kapos, V., Almeida, F., Roberts, D.A., Smith, M.O. and Gillespie, A.R. (1995). Classification of multispectral images based on fractions of endmembers: application to land cover change in the Brazilian Amazon. *Remote Sensing of Environment,* 52, 137-154.

Alavi, M. (1980). Tectonostratigraphic evolution of the Zagros-sides of Iran. *Geology*, 8, 144-149.

Alavi, M. (1994). Tectonic of the Zagros orogenic belt of Iran: new data and interpretations. *Tectonophysics* , 229, 211-238.

Amer, R., Kusky, T. and Ghulam, A. (2010). Lithological mapping in the Central Eastern Desert of Egypt using ASTER data. *Journal of African Earth Sciences,* 56, 75-82.

Amer, R., Kusky, T. and El Mezayen, A. (2012). Remote sensing detection of gold related alteration zones of Um Rus Area, Central Eastern Desert of Egypt. *Advances in Space Research* 49, 121-134.

Amidi, S.M. (1984). Geological map of the Saveh quadrangle: Tehran, Geological Survey of Iran, scale 1:250,000.

Anonymous, (1972). Penrose field conference on ophiolites. *Geotimes*, 17, 24-25.

Arvin, M., Paul, T., Robinson, M. (1994). The petrogenesis and tectonic setting of lavas from the Baft Ophiolitic Mélange, southwest of Kerman, Iran Canadian. *Journal of Earth Sciences*, 31(5), 824-834.

Azizi, H., Tarverdi, M.A. and Akbarpour, A. (2010). Extraction of hydrothermal alterations from ASTER SWIR data from east Zanjan, northern Iran. *Advances in Space Research,* 46, 99-109.

Baldridge A.M., Hook, S.J., Grove, C.I. and Rivera, G. (2009). The ASTER spectral library version 2.0. *Remote Sensing of Environment,* 113, 711-715.

Babai, H. A, La Tour, T. E.(1994) Semibrittle and cataclastic deformation of homblende-quartz rocks in a ductile shear zone. *Tectonophysics*, 229, 19–30.

Bedell, R.L. (2001). Geological mapping with ASTER satellite: new global satellite data that is a significant leap in remote sensing geologic and alteration mapping. *Special Publication Geology Society of Nevada,* 33, 329–334.

Bedini, E., Van Der Meer, F. and Van Ruitenbeek, F. (2009). Use of HyMap imaging spectrometer data to map mineralogy in the Rodalquilar caldera, southeast Spain. *International Journal of Remote Sensing*, 30 (2), 327-348.

Bedini, E. (2009). Mapping lithology of the Sarfartoq carbonatite complex, southern West Greenland, using HyMap imaging spectrometer data. *Remote Sensing of Environment*, 113, 1208-1219.

Bedini, E. (2011). Mineral mapping in the Kap Simpson complex, central East Greenland, using HyMap and ASTER remote sensing data. *Advances in Space Research*, 47, 60-73.

Behzadi, H. (1994). Study of Chemichal Composition of Ophiolite Complex in North of Baft. *Ms thesis University of Bahonar, Kerman ,Iran,* 75-145.

Benomar, T.B., Fuling, B. (2005). Improved Geological Mapping Using Landsat-5 TM Data in Weixi Area, Yunnan Province, China. *Geo-spatial Information Science,* 8(2), 110-114.

Berberian, M. and King, G.C. (1981). Towards a paleogeography and tectonic evolution of Iran. *Canadian Journal of Earth Sciences,* 18, 210-265.

Berberian, F. and Berberian, M. (1981). Tectono-plutonic episodes in Iran. In: Gupta, H.K., Delany, F.M. (Eds.), Zagros Hindukosh, Himalaya Geodynamic Evolution. *American Geophysical Union, Washington* DC, 5-32.

Berberian, F., Muir, I.D., Pankhurst, R.J. and Berberian, M. (1982). Late Cretaceous and early Miocene Andean type plutonic activity in northern Makran and central Iran. *Journal of Geological Society of London,* 139, 605-614.

Biggar, S. F., Thome, K. J., McCorkel, J. T. and D'Amico, J. M. (2005). Vicarious calibration of the ASTER SWIR sensor including crosstalk correction. *Proceedings International Society Optical Engineering,* 17, 5882, 5882.

Bishop, C.A., Liu, J.G. and Mason, P.J. (2011). Hyperspectral remote sensing for mineral exploration in Pulang, Yunnan Province, China. *International Journal of Remote Sensing*, 32(9), 2409-2426.

Boardman, J.W. (1989). Inversion of imaging spectrometry data using singular value decomposition. In: *IGARSS'89, 12th Canadian Symposium on Remote Sensing*, 2069-2072.

Boardman, J.W. (1992). Sedimentary facies analysis using imaging spectrometry: a geophysical inverse problem. Unpublished Ph.D. thesis, University of Colorado.

Boardman, J.W. (1993). Automated spectral unmixing of AVIRIS data using convex geometry concepts: in summaries, Fourth JPL Airborne Geoscience Workshop.

Boardman J. W. and Kruse, F. A. (1994). Automated spectral analysis: A geologic example using AVIRIS data, north Grapevine Mountains, Nevada: *in Proceedings, Tenth Thematic Conference on Geologic Remote Sensing, Environmental Research Institute of Michigan, Ann Arbor, MI,* 407-418.

Boardman, J.W., F.A. Kruse. and Green, R.O. (2000). Mapping target signatures via partial unmixing of AVIRIS data. *Summaries, Proceedings of the Fifth JPL Airborne Earth Science Workshop*, 95(1), 23–26.

Boardman, J. W. (1998). Leveraging the high dimensionality of AVIRIS data for improved sub-pixel target unmixing and rejection of false positives: mixture tuned matched filtering. *Summaries of the Seventh Annual JPL Airborne Geoscience Workshop*, *Pasadena, CA*, 55.

Carranza, E.J. and Hall, M. (2002). Mineral mapping with Landsat Thematic Mapper data for hydrothermal alteration mapping in heavily vegetated terrain. *International Journal of Remote Sensing,* 23 (22), 4827-4852.

Casey, J. F., and J. F. Dewey. (1984). Initiation of subduction zones along transform and accreting plate boundaries, triple-junction evolution, and forearc spreading centres: Implications for ophiolitic geology and obduction, in Ophiolites and Oceanic Lithosphere, *Geol. Soc. Spec. Publ.*, 13, 269-290.

Castro, L, A.I. (2004). An assessment on the potential of mapping hydrothermal alteration from ASTER short wavelength infrared image data based on image simulation experiment. Unpublished M. Sc. Thesis. International Institute for Geo-information Science and Earth Observation Enschede, the Netherlands.

Chabrillat, S., Pinet, P.C., Ceuleneer, G., Johnson, P.E. and Mustard, J.F. (2000). Ronda peridotite massif: methodology for its geological mapping and lithological discrimination from airborne hyperspectral data. *International Journal of Remote Sensing*, 21, 2363-2388.

Chang, Q., Jing, L. and Panahi, A. (2006). Principal component analysis with optimum order sample correlation coefficient for image enhancement. *International Journal of Remote Sensing,* 27 (16), 3387–3401.

Chavez, P. S. J., G. L. Berlin, and L. B. Sowers. (1982). Statistical methods for selecting Landsat-MSS ratios. *Journal of Applied Photogrammetric Engineering,* 8, 23-30.

Chen, X., Warner, T.A. and Campagna, D.J. (2007). Integrating visible, near-infrared and short-wave infrared hyperspectral and multispectral thermal imagery for geological mapping at Cuprite, Nevada. *Remote Sensing of Environment,* 110, 344–356.

Chen, J. Y and Reed, I. S.(1987). A detection algorithm for optical targets in clutter: *IEEE Trans. On Aerosp. Electron*. Syst., vol. AES-23, no.1,235- 259

Clark, J. B., Palmer, C. J. and Shaw, W. N. (1983). The diabetic Zucker fatty rat. *Proc. Soc. Exp. Biol. Med,* 173, 68–75.

Clark, R.N. and Roush, T.L. (1984). Reflectance spectroscopy: quantitative analysis techniques for remote sensing applications. *Journal of Geophysical Research,* 89, 6329–6340.

Clark, R.N., King, T.V.V., Klejwa, M. and Swayze, G.A. (1990). High spectral resolution reflectance spectroscopy of minerals. *Journal of Geophysical Research,* 95, 12653-12680.

Clark, R.N., Swayze, G.A., Gallagher, A., Gorelick, N. and Kruse, F.A. (1991). Mapping with imaging spectrometer data using the complete band shape least-squares algorithm simultaneously fit to multiple spectral features from multiple materials. In: *Proceedings, 3rd Airborne Visible/Infrared Imaging Spectrometer (AVIRIS) Workshop*, 2–3.

Clark, R.N., Swayze, G.A., Gallagher, A., King, T.V.V. and Calvin, W.M. (1993). The U.S. Geological Survey, Digital Spectral Library: Version 1: 0.2 to 3.0 microns: U.S. Geological Survey Open File Report 93-592, 134, http://speclab.cr.usgs.gov (August 1999).

Cloutis, E.A. (1996). Hyperspectral geological remote sensing: evaluation of analytical techniques. *International Journal of Remote Sensing*, 17 (12), 2215-2242.

Cock, K. M., Lucas, S. B., Lucas, S., Agness, J., Kadio, A., Gayle, H. D. (1998). Clinical research, prophylaxis, therapy, and care for HIV disease in Africa. *American Jourrnal Public Health*, 83,1385-1389.

Cousins, C. A. And Feringa, G. (1964).The chromited epositosf thew estern belt of the Bushveld omplexin the geologoy of someo re depositisn southern Africa. *Journal of ohannesbu Grge, ologicaSlo ciety of SouthA fricav*, 2, 183-202.

Cousins, C A. (1964). Additional notes on the chromite deposits of the eastern part of the Bushveld Complex. In S. H. Haughton, Ed., The Geology of Some Or Deposits of Southern Africa, *Geology Society S Africa*. (8) 2, 169-182.

Crippen, R. E. (1989). Selection of landsat TM band and band ratio combinations to maximize lithologic information in color composite display. *In procceding of seventh exploration geologyII*, 912-921.

Crosta, A. and Moore, J. (1989). Enhancement of Landsat Thematic Mapper imagery for residual soil mapping in SW Minais Gerais State, Brazil: a prospecting case history in Greenstone belt terrain. In: *Proceedings of the 7th ERIM Thematic Conference Remote sensing for exploration geology*, 1173-1187.

Crosta, A.P., Souza Filho, C.R., Azevedo, F. and Brodie, C. (2003). Targeting key alteration minerals in epithermal deposits in Patagonia, Argentina, Using ASTER imagery and principal component analysis. *International Journal of Remote sensing,* 24, 4233-4240.

Crowley, J.K. and Vergo, N. (1988). Near-infrared reflectance spectra of mixtures of kaolin group minerals: use in clay mineral studies. *Clays and Clay Mineral*, 36(4), 310-316.

Crowley, J.K., Brickey, D.W. and Rowan, L.C. (1989). Airborne imaging spectrometer data of the Ruby Mountains, Montana: mineral discrimination using relative absorption band-depth images. *Remote Sensing of Environment*, 29(2), 121-134.

Crowley, J.K. and Clark, R.N. (1992). AVIRIS study of Death Valley evaporite deposits using least- squares band-fitting methods. In: *Summaries of the Third Annual JPL Airborne Geoscience Workshop*, 29-31.

De Carvalho, O.A. and Meneses, P.R. (2000). Spectral Correlation Mapper (SCM); An Improvement on the Spectral Angle Mapper (SAM). *Summaries of the 9th JPL Airborne Earth Science Workshop, JPL Publication*, 18, p.9.

Drury, S. L. (2001). Servant leadership and organizational commitment: Empirical findings and workplace implications. *Proceedings of the Servant Leadership Research Roundtable*. Retrieved October 5, 2004, from www.regent.edu/acad/sls/publications/journals_and_proceedings/proceedings/servant_leadership_roundtable/pdf/drury-2004SL.pdf.

Dimitrijevic, M.D. (1973). Geology of Kerman region. *Geological Survey of Iran Report,* 52, 334.

Ducart, D.F., Crosta, A.P. and Filio, C.R.S. (2006). Alteration mineralogy at the Cerro La Mina epithermal prospect, Patagonia, Argentina: field mapping, short-wave infrared spectroscopy, and ASTER images. *Economic Geology*, 101, 981-996.

Farhoudi, G. (1978). A comparison of Zagros geology to island arcs. *Journal of Geology,* 86, 323-334.

Fujisada, H. (1995). Design and performance of ASTER instrument. *Proceedings of SPEI, International Society of Optical Engineering,* 2583, 16-25.

Gabr, S., Ghulam, A. and Kusky, T. (2010). Detecting areas of high-potential gold mineralization using ASTER data. *Ore Geology Reviews,* 38, 59-69.

Gad, S., Kusky, T. M. (2006). Lithological mapping in the Eastern Desert of Egypt, the Barramiya area, using Landsat thematic mapper (TM). *Journal of African Earth Sciences*, 44, 196-202.

Gad, S. and Kusky, T. (2007). ASTER spectral ratioing for lithological mapping in the Arabian–Nubian shield, the Neoproterozoic Wadi Kid area, Sinai, Egypt. *Gondwana Research,* 11, 326-335.

Galva˜o L.S., Almeida-Filho, R. and Vitorello, I. (2005). Spectral discrimination of hydrothermally altered materials using ASTER short-wave infrared bands: Evaluation in a tropical savannah environment. *International Journal of Applied Earth Observation and Geoinformation*, 7, 107-114.

Gersman, R., Ben-Dor, E., Beyth, M., Avigad, D., Abraha, M. and Kibreba, A. (2008). Mapping of hydrothermally altered rocks by the EO-1 Hyperion sensor, northern Danakil, Eritrea. *International Journal of Remote Sensing*, 29 (13), 3911-3936.

Ghazi and Hassanipak, (1999). Geochemistry and petrology of subalkaline and alkaline extrusives of Kermanshah ophiolite, Zagros Suture Zone, SW Iran. *Journal of Asian Earth Sciences*, 17, 319-332.

Geological Survey of Iran. (1973). Exploration for ore deposits in Kerman region, report no,Yu/53.

Grebby, S., Naden, J., Cunningham, D. and Tansey, K. (2011). Integrating airborne multispectral imagery and airborne LiDAR data for enhanced lithological mapping in vegetated terrain. *Remote Sensing of Environment*, 115, 214–226.

Gillespie, A., Abrams, M. and Yamaguchi, Y. (2005). Scientific results from ASTER. *Remote Sensing of Environment*, 99, 1.

Girouard, G., Bannari, A., El Harti, A. and Desrochers, A. (2004). Validated Spectral Angle Mapper Algorithm for Geological Mapping: Comparative Study between Quickbird and Landsat-TM. *XXth, ISPRS Congress*.

Gillespie, A.R., Matsunaga, T., Rokugawa, S. and Hook, S.J. (1998). Temperature and emissivity separation from Advanced Spaceborne Thermal Emission and Reflection Radiometer (ASTER) images. *IEEE Transactions on Geoscience and Remote Sensing 36*, 1113-1126.

Gomez C., Delacourt, C., Allemand, P., Ledru, P. and Wackerle, R. (2005). Using ASTER remote sensing data set for geological mapping, in Namibia. *Physics and Chemistry of the Earth*, 30, 97-108.

Goetz, A.F. H., Rock, B. N. and Rowan, L.C. (1983). Remote sensing for exploration: An overview. *Economic Geology*, 78, 573–590.

Goetz, A. F. H. (2009). Three decades of hyperspectral remote sensing of the Earth: A personal view. *Remote Sensing of Environment,* 113, S6-S16.

Green, A. A., Berman, M., Switzer, P. and Craig, M. D. (1988). A transformation for ordering multispectral data in terms of image quality with implications for noise removal. *IEEE Transactions of Geosciences and Remote Sensing,* 26(1), 65-74.

Green, R.O., Pavri, B.E. and Chrien, T.G. (2003). On-Orbit Radiometric and Spectral Calibration Characteristics of EO-1 Hyperion Derived With an Underflight of AVIRIS and *In Situ* Measurements at Salar de Arizaro, Argentina. *IEEE Transactions of Geosciences and Remote Sensing,* 41(6).

Grove, C. I., Hook, S. J. and Paylor, E. D. (1992). Laboratory reflectance spectra for 160 minerals 0.4 -2.5 micrometers. *Jet Propulsion Laboratory, Pasadena, CA.* 92-2.

Harsanyi, J.C., Farrand, W.H. and Chang, C.I. (1994). Detection of subpixel signatures in hyperspectral image sequences. *Proceedings of 1994 ASPRS Annual Conference,* Reno, Nevada, 236-247.

Hajian, H. (1977). Geological map of the Tafresh area: Tehran, Geological Survey of Iran, scale 1:100,000.

Hashim, M., Pournamdary, M. and BeiranvndPour, A. (2011). Processing and interpretation of advanced space-borne thermal emission and reflection radiometer (ASTER) data for lithological mapping in ophiolite complex. *International Journal of the Physical Sciences*,6 (28), 6410-6421.

Hassanipak, A. M., Ghazi, M. (1999). Petrology, geochemistry and tectonic setting of the Khoy ophiolite, Northwest Iran. *Journal of Asian Earth Sciences*, 18, 43–55.

Hassanzadeh, J. (1993). Metallogenic and tectonomagmatic events in the SE sector of the Cenozoic active continental margin of central Iran (Shahr e Babak area, Keman Province) Ph.D. thesis, University of California, Los Angeles, 204.

Hecker, C., Van der Meijid, M. and Van der Meer, F. (2010). Thermal infrared spectroscopy on feldspar-successes, limitation and their implications for remote sensing. *Earth-Science Reviews*, 103, 60-70.

Hellman M.J and Ramsey M.S. (2004). Analysis of hot springs and associated deposits in Yellowstone National Park using ASTER and AVIRIS remote sensing. *Journal of Volcanology and Geothermal Research,* 135, 195- 219.

Hewson, R.D., Cudahy, T.J. and Huntington, J.F. (2001). Geological and alteration mapping at Mt Fitton, South Australia, using ASTER satellite-borne data. *IEEE Transactions of Geosciences and Remote Sensing*, 724-726.

Hewson, R.D., Cudahy T.J., Mizuhiko, S., Ueda, K. and Mauger, A.J. (2005). Seamless geological map generation using ASTER in the Broken Hill–Curnamona province of Australia. *Remote Sensing of Environment*, 99, 159-172.

Hosseinjani, M. and Tengestani, M.H. (2011). Mapping alteration minerals using sub-pixel unmixing of ASTER data in the Sarduiyeh area, SE Kerman, Iran. *International Journal of Digital Earth*, 4 (6), 487-504.

Hubner, H. (1969a). Geological map of Iran sheet no. 5, southcentral Iran: *Tehran, National Iranian Oil Company*, scale 1:1,000,000.

Hubner, H. (1969b). Geological map of Iran sheet no. 6, southeast Iran: *Tehran, National Iranian Oil Company*, scale 1:1,000,000.

Hunt, G.R., Salisbury, J.W. and Lenhoff, C.J., (1970). Visible and near-infrared spectra of minerals and rocks: III. Oxides and hydroxides. *Modern Geology*, 2, 195–205.

Hunt, G.R., Salisbury, J.W. and Lenhoff, C.J., (1971). Visible and near-infrared spectra of minerals and rocks: IV. Sulphides and sulphates. *Modern Geology*, 3, 1–14.

Hunt, G. R. and Salisbury, J. W. (1974). Mid-infrared spectral behavior of igneous rocks. Technical Report AFRCL-TR-75-0356, US Air Force Cambridge Research Laboratory, Cambridge, MA.

Hunt, G. R. and Salisbury, J. W. (1975). Mid-infrared spectral behavior of sedimentary rocks. Technical Report AFRCL-TR-75-0356, US Air Force Cambridge Research Laboratory, Cambridge, MA.

Hunt, G. R. and Salisbury, J. W. (1976). Mid-infrared spectral behavior of metamorphic rocks, Technical Report AFRCL-TR-76-0003, US Air Force Cambridge Research Laboratory, Cambridge, MA.

Hunt, G. R (1977). Spectral signatures of particulate minerals in the visible and near infrared. *Geophysics,* 42, 501-513.

Hunt, G, R. and Ashley, P. (1979). Spectra of altered rocks in the visible and near infrared. *Economic Geology,* 74, 1613-1629.

Hunt, G. R. and Evarts, P. (1980). The use of near-infrared spectroscopy to determine the degree of serpentinization of ultramafic rocks Geophysics. *Economic Geology,* 46(3), 316–321.

Hunter, E.L. and Power, C.H. (2002). An Assessment of Two Classification Methods *Journal of Remote Sensing,* 23(15), 2989-3008.

Huntington, J.F. (1996). The role of remote sensing in finding hydrothermal mineral deposits on Earth. Evolution of Hydrothermal Ecosystems on Earth (and Mars?). *Wiley England*, 214-234.

Inzana, J., Kusky, T., Higgs, G. and Tucker, R. (2003). Supervised classifications of Landsat TM band ratio images and Landsat TM band ratio image with radar for geological interpretations of central Madagascar. *Journal of African Earth Sciences*, 37, 59-72.

Iwasaki, A. and Tonooka, H. (2005). Validation of a crosstalk correction algorithm for ASTER/SWIR. *IEEE Transactions Geoscience and Remote Sensing*, 43(12), 2747-2751.

James, K., Vergo, C. and Vergo, N. (1988). Near-infrared reflectance spectra of mixtures of kaolin-group minerals: use in clay mineral studies. *Clay and Clay Minerals*, 36(4), 310-316.

Jankovic, S. (1984). Metallogeny of the Alpine granitoids in the Tethyan-Eurasian metallogenic belt. *Proceedings of the 27th International Geological Congress, Moscow, 4-14 August, 1984*, 247-274.

Jensen, J.R. (2005). Introductory Digital Image Processing. Pearson Prentice Hall, Upper Saddle River. *International Journal of Remote Sensing,23, 514-527.*

Junek, P. (2004). Geological mapping in the Cheleken Peninsula, Turkministan area using Advanced Spaceborne Thermal Emission and Reflection Radiometer (ASTER) data. *ISPRS Conference*, *May 2004, California*, USA.

Kanlinowski, A. and Oliver, S. (2004). ASTER Mineral Index Processing. Remote Sensing Application Geoscience Australia. Australian Government Geoscience Website: http://www.ga.gov.au/image_cache/GA7833.pdf , access date 20 June 2010.

Kang, Q., Rong, Y., Xiangjun, L. and Xiaolian, D. (2005). Application of spectral angle mapping model to rapid assessment of soil salinization in arid area. *IEEE Transactions of Geosciences and Remote Sensing*, 2355-2357.

Kavak, K.S. (2005). Recognition of gypsum geohorizons in the Sivas Basin (Turkey) using ASTER and Landsat ETM+ images. *International Journal of Remote Sensing,* 26, (20), 4583-4596.

Kevin, w., Walden, J., Drake, N.A., Eckardt, F. and Settle, J.J. (1997). Mapping the iron oxide content of dune sands, Namib sand sea, Namibia, using Landsat Thematic Mapper data. *Remote Sensing of Environment*, 62, 30-39.

Khan S.D., Mahmood, K. and Casey, J.F. (2006). Mapping of Muslim Bagh ophiolite complex (Pakistan) using new remote sensing, and field data. *Journal of Asian Earth Sciences,* 30, 333-343.

Khan, S. D. and Mahmood, K. (2008). The application of remote sensing techniques to the study of ophiolites. *Earth-Science Reviews,* 89, 135-143.

Klein, C. (1962). Diagram 23: Equilibrium distribution of chromium species in water at 25'C and one atmosphere total pressure. In, H. H. Schmitt, Jr., Ed., Equilibrium Diagrams for Minerals at Low Temperature and Pressure. *The Geological Club of Harvard,* 116 (19), 236-257.

Klein, U, Sharp, T. G, Schumacher, J. C. (1993). Analytical elec- tron microscopy of nanometer-scale hornblende lamellae: low-temperature exsolution in cummingtonite. *Am. Mineral.* 82, 1079–1090.

Kratt, C., Calvin, W. M. and Coolbaugh, M. F. (2010). Mineral mapping in the Pyramid Lake basin: Hydrothermal alteration, chemical precipitates and geothermal energy potential. *Remote Sensing of Environment,* 114 (10), 2297-2304.

Krohn, M.D., Abrams, M.J. and Rowan, L.C. (1978). Discrimination of hydrothermal altered rocks along the Battle Mountain–Eureka, Nevada, mineral belt using Landsat images: *U.S. Geological Survey Open-File Report,* 78,585-594.

Kruse, F.A., Boardman, J.W., Lefkoff, A.B., Heidebrecht, K.B., Shapiro, A.T., Barloon, P.J. and Goetz, A.F.H. (1993). The Spectral Image Processing System (SIPS) – Interactive Visualization and Analysis of Imaging Spectrometer Data. *Remote Sensing of Environment,* 44, 145-163.

Kruse, F. A. and Lefkoff, A. B. (1993). Knowledge-based geologic mapping with imaging spectrometers: *Remote Sensing Reviews, Special Issue on NASA Innovative Research Program (IRP) results*, 8, 3 -28.

Kruse, F. A., Boardman, J. W. and Huntington, J. F. (1999). Fifteen Years of Hyperspectral Data: Northern Grapevine Mountains, Nevada: in *Proceedings of the 8th JPL Airborne Earth Science Workshop*: Jet Propulsion Laboratory Publication, JPL Publication, 99 (17), 247- 258.

Kruse, F.A and Boardman, J. W. (2000). Characterization and Mapping of Kimberlites and Related Diatremes Using Hyperspectral Remote Sensing. *Proceedings, 2000 IEEE Aerospace Conference., Big Sky, MO*, March 18-24.

Kruse, F.A., Bordman, J.W. and Huntington, J.F. (2003). Comparison of airborne hyperspectral data and EO-1 Hyperion for mineral mapping. *IEEE Transactions of Geosciences and Remote Sensing*, 41(6), 1388-1400.

Kruse, F. A., Perry, S.L. and Caballero, A. (2006). District-level mineral survey using airborne hyperspectral data, Los Menucos, Argentina. *Annals of Geophysics*, 49 (1), 83-92.

Kruse, F. A. and Perry, S.L. (2007). Regional mineral mapping by extending hyperspectral signatures using multispectral data. *IEEE Transactions of Geosciences and Remote Sensing*, 4, 1-14.

Kusky T, M. and Ramadan, T.M. (2002). Structural controls on Neoproterozoic mineralization in the South Eastern Desert, Egypt: an integrated field, Landsat TM, and SIR-C/X SAR approach. *Journal of African Earth Sciences,* 35, 107-121.

Leverington, W.D. (2012). Landsat-TM-Based Discrimination of Lithological Units Associated with the Purtuniq Ophiolite, Quebec, Canada.*journal of remote sensing,* 4, 1208-1231.

Lippard, S.J., Selton, A.W., Gass, I.G.(1986) The ophiolite of northern Oman. *Blackwell Oxford,* 178,965 983.

Lorenz, R. D., Niemann, H. B., Harpold, D. N., Way, S. H. and Zarnecki, J. C. (2006). Titan's damp ground: Constraints on Titan surface thermal properties from the temperature evo- lution of the Huygens GCMS inlet. *Meteoritics and Plane- tary Science*, 41, 1705-1714.

Loughlin, W. P. (1991). Principal component analysis for alteration mapping; *journal of Photogrammetric Engineering and Remote Sensing*, 57, 1163–1169.

McCall, G. (1997). The geotectonic history of the Makran and adjacent areas of southern Iran. *Journal of Asian Earth Sciences* 15(6), 517-531.

Madani, A. A. and A. A. Emam (2011). "SWIR ASTER band ratios for lithological mapping and mineral exploration: A case study from El Hudi area, southeastern desert, Egypt." *Arabian Journal of Geosciences* 4(1), 45-52.

Malekizadeh, A. (1999). Geochemistry and petrogenesis of granite batholiths of Siah Kuh plutonic complex. Unpublished MSc thesis, Shahid Bahonar University, Kerman, I.R. Iran, 208.

Mars, J. C. and Rowan, L.C. (2006). Regional mapping of phyllic- and argillic-altered rocks in the Zagros magmatic arc, Iran, using Advanced Spaceborne Thermal Emission and Reflection Radiometer (ASTER) data and logical operator algorithms. *Geosphere,* 2(3), 161-186.

Mars, J.C. and Rowan, L.C. (2007). Mapping sericitic and argillic-altered rocks in southeastern Afghanistan using Advanced Spaceborne Thermal Emission and Reflection Radiometer (ASTER) data, U.S. Geological Survey Open-File Report 2007–1006, 1 plate, http://pubs.usgs.gov/of/2007/1006/.

Mars, J. C. and Rowan, L.C. (2010). Spectral assessment of new ASTER SWIR surface reflectance data products for spectroscopic mapping of rocks and minerals. *Remote Sensing of Environment,* 114, 2011-2025.

Mars, J. C. and Rowan, L.C. (2011). ASTER spectral analysis and lithologic mapping of the Khanneshin carbonate volcano, Afghanistan. *Geosphere,* 7, 276-289.

Massironi, M. L., Bertoldi, P., Calafa, D., Visona, A., Bistacchi, C., Giardino, A. and Schiavo, B. (2008). Interpretation and processing of ASTER data for geological mapping and granitoids detection in the Saghro massif (eastern Anti-Atlas, Morocco). *Geosphere,* 4(4), 736 -759.

Matthews, J. P. and Jones, A. S. G. (1992). Mapping the Xigaze(Tibet) ophiolite complex with Landsat Thematic Mapper data. *Journal of Himalayan Geology*, 3, 97-101.

Mezned, N., Abdeljaoued, S. and Boussema, M.R. (2009). A comparative study for unmixing based Landsat ETM+ and ASTER image fusion. *International Journal of Applied Earth Observation and Geoinformation*, 12(1), 131-137.

Mickus, T., Jung, H. Y. and Spruston, N. (1999). Slow sodiumchannel inactivation in CA1 pyramidal cells. *Ann. NY Acad. Sci*, 868, 97–101.

Modarres, R. and Da Silva V. P. R. (2007). Rainfall trends in arid and semi-arid regions of Iran. *Journal of Arid Environments*, 70, 344-355.

Moghtaderi, A., Moore F. and Mohammadzadeh, A. (2007). The application of Advanced Space-borne Thermal Emission and Reflection (ASTER) radiometer data in the detection of alteration in the Chadormalu paleocrater, Bafq region, Central Iran. *Journal of Asian Earth Sciences*, 30, 238–252.

Moore, F., Rastmanesh, F., Asady, H. and Modabberi, S. (2008). Mapping mineralogical alteration using principal component analysis and matched filter processing in Takab area, north-west Iran, from ASTER data. *International Journal of Remote Sensing,* 29, (10), 2851-2867.

Myint Soe., Toe Aung Kyaw. and Isao Takashima. (2005). Application of Remote Sensing Techniques on Iron Oxide Detection from ASTER and LandsatImages of Tanintharyi Coastal Area, Myanmar. *Journal of Gastroenterol*, 13, 225–235.

Nalbant, S., and Alptekin, O., (1995). The use of Landsat Mapper imagery for analyzing lithology and structure of Korucu-DuZla area in western Turkey: *International Journal of Remote Sensing,* 10, 2337-2374.

Ninomiya, Y., and Fu, B. (2002). Mapping quartz, carbonate minerals and mafic–ultramafic rocks using remotely sensed multispectral thermal infrared ASTER data. *Proceedings of SPIE,* 4710, 191-202.

Ninomiya, Y. (2003a). A stabilized vegetation index and several mineralogic indices defined for ASTER VNIR and SWIR data. *Proc. IEEE 2003 International Geoscience and Remote Sensing Symposium (*IGARSS'03), Toulouse, France, 21–25 July 2003, (3), 1552-1554.

Ninomiya, Y. (2003b). Advanced remote lithologic mapping in ophiolite zone with ASTER multispectral thermal infrared data. *Proc. IEEE 2003 International Geoscience and Remote Sensing Symposium (IGARSS'03)* Toulouse, France, 21–25 July 2003, (3),1561-1563.

Ninomiya, Y. (2003c). Rock type mapping with indices defined for multispectral thermal infrared ASTER data: case studies. *Proceedings of SPIE*, 4886, 123-132.

Ninomiya, Y. (2004). Lithological mapping with ASTER TIR and SWIR data. *Proceedings of SPIE*, 5234, 180-190.

Ninomiya, Y., Fu, B. and Cudahy, T.J. (2005). Detecting lithology with Advanced Spaceborne Thermal Emission and Reflection Radiometer (ASTER) multispectral thermal infrared ‘‘radiance-at-sensor” data. *Remote Sensing of Environment*, 99 (1-2), 127-139.

Okada, K., Segawa, K. and Hayashi, I. (1993). Removal of the vegetation effect from LANDSAT TM and GER imaging spectroradiometer data. *ISPRS Journal of Photogrammetry and Remote Sensing*, 48 (6), 16-27.

Oztan, N.S. and Suzen, M.L. (2011). Mapping evaporate minerals by ASTER. *International Journal of Remote Sensing*, 32 (6), 1651-1673.

Perry, S.L. (2004). Spaceborne and airborne remote sensing systems for mineral exploration-case histories using infrared spectroscopy. In: King, P.L., Ramsey, M.S., Swayze, G.A. (Eds.), Infrared Spectroscopy in Geochemistry, Exploration Geochemistry, and Remote Sensing. Mineralogic Association of Canada, London, Canada, 227-240.

Pohl, C., Van Genderen. (1998). Multisensor image fusion in remote sensing: concepts, methods and applications. International journal of remote sensing, 19 (5), 823- 854.

Pour, B. A., Hashim, M. and Marghany, M. (2011). Using spectral mapping techniques on short wave infrared bands of ASTER remote sensing data for alteration mineral mapping in SE Iran. *International Journal of the Physical Sciences,* 6(4), 917-929.

Pour, B.A. and Hashim, M. (2011a). Identification of hydrothermal alteration minerals for exploring of porphyry copper deposit using ASTER data, SE Iran. *Journal of Asian Earth Sciences*, 42, 1309-1323.

Pour, B. A. and Hashim, M. (2011b). Spectral transformation of ASTER and the discrimination of hydrothermal alteration minerals in a semi-arid region, SE Iran. *International Journal of the Physical Sciences*, 6(8), 2037-2059.

Pour, B. A. and Hashim, M. (2011c). Application of Spaceborne Thermal Emission and Reflection Radiometer (ASTER) data in geological mapping. *International Journal of the Physical Sciences*, 6(33), 7657-7668.

Pour, B. A. and Hashim, M. (2011d). The Earth Observing-1 (EO-1) satellite data for geological mapping, southeastern segment of the Central Iranian Volcanic Belt, Iran. *International Journal of the Physical Sciences,* 6(33), 7638-7650.

Pour, B.A. and Hashim, M. (2012a). The application of ASTER remote sensing data to porphyry copper and epithermal gold deposits. *Ore Geology Reviews*. 44, 1-9.

Pour, B. A. and Hashim, M. (2012b). Identifying areas of high economic-potential copper mineralization using ASTER data in Urumieh-Dokhtar Volcanic Belt, Iran. Advances in Space Research 49, 753-769.

Pournamdari, M. and Hashim. M. (2013). Detection of Chromite Bearing Mineralized Zones In Abdasht Ophiolite Complex Using ASTER And ETM+ Remote Sensing Data, South Of Iran. *Arabian journal of Geosciences, DOI 10.1007/s12517-013-0927-0.*

Qari, M. Y. H. T. (1991). Application of Landsat TM Data to Geological Studies, Al-Khabt Area, Southern Arabian. *Photogrammetric Engineering and Remote Sensing*, 57(4), 421-429.

Qiu, F., Abdelsalam, M. and Thakkar, P. (2006). Spectral analysis of ASTER data covering part of the Neoproterozoic Allaqi-Heiani suture, Southern Egypt. *Journal of African Earth Sciences*, 44, 169–180.

Raines, G.L. (1978). Porphyry copper exploration model for northern Sonora, Mexico. *U.S. Geological Survey Journal of Research*, 6, 51–58.

Rajendran, S., Thirunavukkarasu, A., Balamurugan, G. and Shankar, K. (2011a). Discrimination of iron ore deposits of granulite terrain of Southern Peninsular India using ASTER data. *Journal of Asian Earth Sciences,* 41, 99–106.

Rajendran, S., Al-Khirbasha S., Pracejusa, B., Nasira, S., Al-Abria, A. H., Kusky, T.M. and Ghulam, A. (2012). ASTER detection of chromite bearing mineralized zones in Semail Ophiolite Massifs of the northern Oman Mountains: Exploration strategy. *Ore Geology Reviews*, 44, 121-135.

Rajesh, H.M. (2008). Mapping Proterozoic unconformity-related uranium deposits in the Rockole area, Northern Territory, Australia using Landsat ETM+. *Ore Geology Reviews*, 33, 382-396.

Ramadan, T.M. and Abdel Fattah, M.F. (2010). Characterization of gold mineralization in Garin Hawal area, Kebbi State, NW Nigeria, using remote sensing. *The Egyptian Journal of Remote Sensing and Space Science*, 13, 153-163.

Ranjbar, H., Masoumi, F. and Carranza, E.J.M. (2011). Evaluation of geophysics and spaceborne multispectral data for alteration mapping in the Sar Cheshmeh mining area, Iran. *International Journal of Remote Sensing,* 32 (12), 3309-3327.

Raziei, T., Daneshkar, P., Arasteh, R. and Saghfian, B. (2005). Annual Rainfall Trend in Arid and Semi-arid Regions of Iran. *ICID 21st European Regional Conference* 2005- 15-19 May 2005, Frankfurt (Oder) and Slubice - Germany and Poland.

Ren, D. and Abdelsalam, M.G. (2006). Tracing along-strike structural continuity in the Neoproterozoic Allaqi-Heiani Suture, southern Egypt using principal component analysis (PCA), fast Fourier transform (FFT), and redundant wavelet transform (RWT) of ASTER data. *Journal of African Earth Sciences*, 44, 181–195.

Robinson, J., Beck, R. (2000). New structural and stratigraphic insight for northwestern Pakistan from field and Landsat thematic mapper data. *Geological Society of America Bulletin*, 112, 364-374.

Rockwell, B. W. and Hofstra, A.H. (2008). Identification of quartz and carbonate minerals across northern Nevada using ASTER thermal infrared emissivity data, implications for geologic mapping and mineral resource investigations in well-studied and frontier areas. *Geosphere,* 4 (1), 218–246.

Rothery, D. A. (1987). Improved discrimination of rock units using Landsat Thematic Mapper imagery of the Oman ophiolite. *Journal of Geologic Society London*, 144, 587-597.

Routschka, G. (2008). Pocket manual refractory materials, *Vulkan-Verlag GmbH.*

Rowan, L.C., Wetlaufer, P.H., Goetz, A.F.H., Billingsley, F.C. and Stewart, J.H. (1974). Discrimination of rock types and detection of hydrothermally altered areas in south-central Nevada. *U.S. Geological Survey Professional Paper*, 35, 883.

Rowan, L.C., Goetz, A.F.H. and Ashley, R.P. (1977). Discrimination of hydrothermally altered and unaltered rocks in visible and near infrared multispectral images. *Geophysics,* 42 (3), 522-535.

Rowan, L.C. and Wetlaufer, P.H. (1981). Relation between regional lineament systems and structural zones in Nevada. American Association of Petroleum Geologists Bulletin, 65, 1414–1432.

Rowan, L.C. and Mars, J.C. (2003). Lithologic mapping in the Mountain Pass, California area using Advanced Spaceborne Thermal Emission and Reflection Radiometer (ASTER) data. *Remote Sensing of Environment*, 84, 350-366.

Rowan, L.C., Hook, S.J., Abrams, M.J. and Mars, J.C. (2003). Mapping hydrothermally altered rocks at Cuprite, Nevada, using the Advanced Spaceborne Thermal Emission and Reflection Radiometer (ASTER), a new satellite-imaging system. *Economic Geology*, 98(5), 1019-1027.

Rowan, L.C., Mars, J.C. and Simpson, C.J. (2005). Lithologic mapping of the Mordor N.T, Australia ultramafic complex by using the Advanced Spaceborne Thermal Emission and Reflection Radiometer (ASTER). *Remote Sensing of Environment*, 99, 105-126.

Rowan, L.C, Robert G. S. and John C. (2006). Distribution of hydrothermally altered rocks in the Reko Diq, Pakistan mineralized area based on spectral analysis of ASTER data. *Remote Sensing of Environment,* 104, 74-87.

Rowins, S.M. (1999). Reduced porphyry copper-gold deposits: a newly recognized style of gold mineralization. *Geological Society of American Abstract with program*, 31(7), A92.

Sabins, F.F. (1987). *Remote Sensing Principles and Interpretation*. 2ned Freeman, New York.

Sabins, F.F. (1996). *Remote Sensing Principles and Interpretation*, third ed. Freeman & Co, New York, USA.

Sabins, F.F. (1997). Remote sensing strategies for mineral exploration. In: Rencz, A.E. (Ed.), *Remote Sensing for the Earth Sciences John Wiley & Sons, Inc.*, New York, 375-447.

Sabins, F.F. (1999). Remote sensing for mineral exploration. *Ore Geology Reviews,* 14, 157-183.

Sabzehie, M., Watters, M. (1970). Preliminary report on the geology and petrography of the metamorphic and igneous rocks of central partof Neiriz. *Geological Survey of Iran*, 236-432.

Sabzehie, M. (1995). Geological Quadrangle Map of Iran, No. 12, Hajiabad, 1:250,000, First compilation by Berberian, M. and Final compilation and revision by Sabzehei, M., *Geological Survey of Iran*.

Salati, S., Van Ruitenbeek, F.J.A., Van der Meer, F.D., Tangestani, M.H. and Van der Werff, H. (2011). Lithological mapping and fuzzy set theory: Automated extraction of lithological boundary from ASTER imagery by template matching and spatial accuracy assessment. *International Journal of Applied Earth Observation and Geoinformation*, 13, 753-765.

Sanjeevi, S. (2008). Targeting limestone and bauxite deposits in Southern India by spectral unmixing of hyperspectral image data. *The International Archives of Photogrammetry, Remote Sensing and Spatial Information Sciences*.235-246.

Saric, V. and Mijalkovic, N. (1973). Metallogenic map of Kerman region, 1:500000 scale. In: Khadem, N., Nedimovic, R. (Eds.), Exploration for Ore Deposits in Kerman Region. *Geological Survey of Iran Report*, 53, 247.

Scheidt, S., Ramsey, M. and Lancaster, N. (2008). Radiometric normalization and image mosaic generation of ASTER thermal infrared data: An application to extensive sand and dune fields. *Remote Sensing of Environment*, 112(3), 920–933.

Sengor, A.M.C. (1991). Late Paleozoic and Mesozoic evolution of the Middle Eastern Tethysides: Implications for the Paleozoic Geodynamics of the Tethyan Realm. *IGCP Project 276, Newsletter No. 2*, III-149.

Shahabpour J. (2005). Tectonic evolution of the orogenic belt in the region located between Kerman and Neyriz. *Journal of Asian Earth Sciences*, 24, 405 -417.

Shahabpour J. and Alavi M. (2007). Island-arc affinity of the Central Iranian Volcanic Belt. *Journal of Asian Earth Sciences*, 30, 652-665.

Shervais, J. W. (1993) Tectonic implications of oceanic basalts in the Coast Range ophiolite, California: Evidence for ridge subduction as final ophiolite-forming event, *Geol. Soc. Am. Abstr. Programs*, 25 (6), 445.

Shimabukuro, Y.E., and Smith, J.A. (1991). The least-squares mixing models to generate fraction images derived from remote sensing multispectral data. IEEE Transactions of Geosciences and Remote Sensing, 29, 16-20.

Singh, A. and Harrison, A. (1985). Standardized principal components. *International Journal of Remote Sensing*, 6, 883–896.

Stocklin, J. and Nabavi, M.H. (1973). Tectonic Map of Iran, 1:2,500,000, *Geological Survey of Iran.*

Stocklin, J. (1974). Possible ancient continental margins in Iran. In: Burk, C.A., Drake, C.L. (Eds.), The Geology of Continental Margins, Springer, Berlin, 873-887.

Stocklin, J. (1977). Structural correlation of the Alpine range between Iran and Central Asia. *Me´moire Hors-Se´rve No. 8 dela Socie´te´ Geologique de France* 8, 333-353.

Stocker, R.F., Lienhard, M.C., Borst, A., Fischbach, K.F. (1990). Neuronal architecture of the antennal lobe in Drosophila melanogaster. *Cell Tissue Res*. 262 (1): 9-34

Sultan, M., Arvidson, R.E. and Sturchio N.C. (1986). Mapping of serpentinites in the Eastern Desert of Egypt using Landsat Thematic Mapper data. *Geology*, 14, 995-999.

Sultan, M., Arvidson, R.E., Sturchio. N.C. and Guinness, E.A. (1987). Lithologic mapping in arid regions with Landsat thematic mapper data: Meatiq Dome, Egypt. *Geological Society of America Bulletin,* 99 (6), 748-762.

Swayze, G.A. and Clark, R.N. (1995). Spectral identification of minerals using imaging spectrometry data: evaluating the effects of signal to noise and spectral resolution using the Tricorder Algorithm. In: *Summaries of the Fifth Annual JPL Airborne Earth Science Workshop*, 157-158.

Tangestani, M. H., Mazhari, N., Ager, B. and Moore, F. (2008). Evaluating advance spaceborne thermal emission and reflection radiometer (ASTER) data for alteration zone enhancement in a semi-arid area, northern shahr-e-Babak, SE Iran. *International Journal of Remote Sensing,* 29(10), 2833-2850.

Tangestani, M.H., Jaffari, L., Vincent, R.K. and Sridhar, B.B.M. (2011). Spectral characterization and ASTER-based lithological mapping of an ophiolite complex: A case study from Neyriz ophiolite, SW Iran. *Remote Sensing of Environment*, 115, 2243-2254.

Thome, K., Palluconi, F., Takashima, T. and Masuda, K. (1998). Atmospheric Correction of ASTER. *IEEE Transactions of Geosciences and Remote Sensing,* 36(4), 1119-1211.

Thome, K.J., Biggar, S.F. and Wisniewski, W. (2003). Cross Comparison of EO-1 Sensors and Other Earth Resources Sensors to Landsat-7 ETM+ Using Railroad Valley Playa. *IEEE Transactions of Geosciences and Remote Sensing*, 41(6).

Van der Meer, F., Vasquez-Torres, M. and Van Dijk, P.M. (1997). Spectral Characterization of Ophiolite Lithologies in the Troodos Ophiolite Complex of Cyprus and its Potential in prospecting for Massive Sulphide Deposits. *International Journal of Remote Sensing,* 18(6), 1245-1257.

Van der Meer, F. and De Jong, S.M. (2000). Improving the results of spectral unmixing of Landsat thematic mapper imagery by enhancing the orthogonality of end-member. *International Journal of Remote Sensing,* 21(15), 2781-2797.

Van der Meer, F.D., Van der Werff, H.M.A., Van Ruitenbeek, F.J.A., Hecker, C.A., Bakker, W.H., Noomen, M.F., Van der Meijde, M., Carranza, E. J.M., Boudewijn de Smeth, J. and Woldai, T. (2012). Multi- and hyperspectral geologic remote sensing: A review. *International Journal of Applied Earth Observation and Geoinformation*, 112-128.

Velosky, J.C., Stern, R.J. and Johnson, P.R. (2003). Geological control of massive sulfide mineralization in the Neoproterozoic Wadi Bidah shear zone, southwestern Saudi Arabia, inferences from orbital remote sensing and field studies. *Precambrian Research,* 123 (2-4), 235-247.

Vicente, L.E. and Filho C.R.S. (2011). Identification of mineral components in tropical soils using reflectance spectroscopy and advanced spaceborne thermal emission and reflection radiometer (ASTER) data. *Remote Sensing of Environment*, 115, 1824–1836.

Watts, D.R. and Harris, N.B. W. (2005). Mapping granite and gneiss in domes along the North Himalayan antiform with ASTER SWIR band ratios. *Geological Society of America Bulletin*, 117(7/8), 879-886.

Williams, H. and Smyth, W. R. (1973). Metamorphic aureoles beneath ophiolite suites and Alpine peridotites: tectonic implications with west Newfoundland examples. *American Journal of Science*, 273, 594–621.

Wickert, L.M. and Budkewtisch, P. (2004). ASTER a geological mapping tool for Canada's north. Case study: the Becher Island, Hudson Bay, Nunavut, Canada. *IEEE Transactions of Geosciences and Remote Sensing*, 1300-1303.

Wolfe, J.A. (1998). Arc magmatism and mineralization in North Luzon and its relationship to subduction at the East Luzon and North Manila Trenches. *Southeast Asian Earth Sciences*, 2(2), 79-93.

Xiong, M., Breen, A., Bisi, M., Owens, M., Fallows, R., Dorrian, G., Davies, J., Thomasson, P. (2011). Forward modelling to determine the observational signatures of white-light imaging and interplanetary scintillation for the propagation of an interplanetary shock in the ecliptic plane. *Journal of Atmospheric Solar-Terr.Physic*, 73, 1270 – 1280.

Xu, Y., Qizhong, L., Shao, Y. and Wang, L. (2004). Extraction Mechanism of Alteration Zones using ASTER Imagery. *Geosciences and Remote Sensing Symposium, IGARSS 04, Proceedings 2004 IEEE International,* 6, 4174-4175.

Yamaguchi Y.I., Fujisada, H., Kudoh, M., Kawakami, T., Tsu, H., Kahle, A.B. and Pniel, M. (1999). ASTER instrument characterization and operation scenario. *Advanced Space Research*, 23(8), 1415-1424.

Yamaguchi Y.I., Fujisada, H., Kahle, A.B., Tsu, H., Kato, M., Watanabe, H., Sato, I. and Kudoh, M. (2001). ASTER instrument performance, operation status, and application to Earth sciences. *IEEE Transactions of Geosciences and Remote Sensing*, 1215-1216.

Yamaguchi, Y. and Naito, C. (2003). Spectral indices for lithologic discrimination and mapping by using the ASTER SWIR bands. *International Journal of Remote Sensing,* 24(22), 4311-4323.

Yesou, H., Y. Besnus, and J. Rolet. (1993). Extraction of spectral information from Landsat TM data and merger with SPOT panchromatic imagery contribution to the study of geological structures. *ISPRS Journal of Photogrammetry and Remote Sensing,* 48(5), 23–36.

Yuhas, R.H., Goetz, A.F.H. and Boardman, J.W. (1992). Discrimination among semi-Arid landscape endmembers using the Spectral Angle Mapper (SAM) Algorithm. *Summaries of the 4th JPL Airborne Earth Science Workshop, JPL Publication*, 92-41, 147-149.

Zhang, X., Pazner, M. and Duke, N. (2007). Lithologic and mineral information extraction for gold exploration using ASTER data in the south Chocolate Mountains (California). *Journal of Photogrammetry and Remote Sensing*, 62, 271-282.

Zhang, X. and Pazner, M. (2007). Comparison of Lithologic Mapping with ASTER, Hyperion and ETM Data in the Southeastern Chocolate Mountains, USA. *Photogrammetric Engineering and Remote Sensing,* 73(5), 555-561.

Zhang, X. (2010). Multi-source remote sensing data fusion: status and trends. *International Journal of Image and Data Fusion,*1(1) 5–24.

Zoheir, B. and Emam, A. (2012). Integrating geologic and satellite imagery data for high-resolution mapping and gold exploration targets in the South Eastern Desert, Egypt. *Journal of African Earth Sciences*, 66-67, 22-34.